Rhamnolipids from the Rhizosphere Bacterium *Pseudomonas* sp. GRP_3 That Reduces Damping-off Disease in Chilli and Tomato Nurseries

Alok Sharma,[†,§] Rolf Jansen,[‡] Manfred Nimtz,[†] Bhavdish N. Johri,[§] and Victor Wray*[,†]

Department of Structural Biology and Research Group Microbial Drugs, Helmholtz Centre for Infection Research (HZI), Braunschweig, Germany, and Department of Microbiology, CBS&H, GB Pant University of Agriculture & Technology, Pantnagar 263145, India

Received January 3, 2007

A detailed screening of bacterial isolates from the Central Himalayan region for plant growth promotion and antimycelial activity against *Pythium* and *Phytophthora* strains afforded seven isolates, of which three were particularly effective against the incidence of damping-off in field trials on chilli and tomato. In this investigation an initial spectroscopic survey of the methanolic extracts of the seven bacterial isolates showed complex mixtures except for *Pseudomonas* sp. GRP_3, one of the most promising isolates on the basis of field studies. Strain GRP_3 was selected for structural characterization of its secondary metabolites, particularly glycolipids. The extracellular secondary metabolites were enriched by Amberlite XAD-16 adsorber resin followed by separation and structural analysis using TLC, LC-MS, MS-MS, and NMR spectroscopy. Acquired data show the presence of a number of mono- and dirhamnolipids and include rhamnose (Rha)-C8-C10, Rha-C10-C8, Rha-C10-C10, Rha-C10-C12:1, Rha-C10-C12, Rha-Rha-C8-C10, Rha-Rha-C10-C10, Rha-Rha-C10-C10:1, Rha-Rha-C10-C12, Rha-Rha-C10-C12:1, Rha-Rha-C12-C12:1, and Rha-Rha-C12-C12 in strain GRP_3. Since rhamnolipids are involved in the lysis of the plasma membrane of zoospores of fungi, application of such rhamnolipid-producing rhizobacteria could facilitate control of damping-off plant pathogens.

Bacterial diversity present in the rhizosphere not only is crucial for growth of crop plants but also determines natural mechanisms of disease control. In this context the fluorescent pseudomonads are favored in ecologically based crop management and soil health by virtue of their rapid root and rhizosphere colonization capacity, utilization of a wide variety of molecules as growth substrates,[1,2] and release of secondary metabolites that are crucial to indigenous competition and growth promotory compounds that help improve root proliferation and consequent plant growth.[3]

Pseudomonad-mediated disease suppression is a consequence of the synthesis of a great diversity of primary and secondary metabolites, many of which are released into the surrounding environment. One of the major mechanisms is related to the secretion of antibiotics such as pyoluteorin, pyrrolnitrin, phenazine-1-carboxylic acid, and 2,4-diacetylphloroglucinol (DAPG).[2,4,5,6] However, restricted rhizosphere competence and root colonization potential make their natural performance variable. For example, in a plant growth dependent study of DAPG producers in the maize rhizosphere, only 188 out of a total of 1716 isolates were positive for this antibiotic.[7] Plant growth promoting rhizobacteria (PGPR) also produce iron-chelating siderophores and affect plant growth via lowering the iron status in the root zone for phytopathogens, thus inhibiting their colonization[8] but may offer iron to plants through heterologous iron uptake.[9] In addition *Pseudomonas* are able to produce glycolipids, in particular rhamnolipids, that act as biosurfactants and can be applied successfully against zoosporic plant pathogens.[10−12]

In an ongoing research program we have recently screened a large collection of fluorescent pseudomonads and other rhizobacteria for plant growth promoting and antimycelial activity against three damping-off pathogens, namely, two *Pythium aphanidermatum* strains and *Phytophthora nicotianae*, originally obtained from the Indian Culture Collection, New Delhi.[13] Seven bacterial isolates (*Pseudomonas* sp. 146, D4, H3, FQP PB-3, FQA PB-3, GRP_3 and isolate SH 1U-13, originating from various habitats in the Central Himalayan region[13]) were selected, and their effectiveness in field trials for combating pre- and post-emergence damping-off in tomato and chilli (also called chile) was assessed under natural and artificially disease-infested field sites in both winter and wet seasons. Three isolates, namely, FQP PB-3, FQA PB-3, and GRP_3, were particularly beneficial. On the basis of this and earlier studies[8,14,15] with strain GRP_3, we have now performed an initial nuclear magnetic resonance (NMR) spectroscopic screening of the secondary metabolite profile of the seven bacterial isolates and have selected GRP_3 for rhamnolipid characterization. Here, we report a detailed structural characterization of the extracellular secondary metabolites produced by GRP_3 using mass spectrometry (MS) and NMR spectroscopy.

Results and Discussion

The diversity of microflora associated with the plant rhizosphere is influenced considerably by the surrounding biotic and abiotic factors. Among the biotic factors, bacteria, fungi, protozoa, and nematode populations either directly or indirectly influence plant health and productivity.[1,3] Within this scenario, the most well-studied phenomenon is the antagonistic activity of rhizosphere microorganisms toward plant pathogens with the resultant suppression of plant disease.[2,5] Plant growth promoting rhizobacteria (PGPR) offer a valid alternative to costly synthetic pesticides to check proliferation of soil-born plant pathogens and simultaneously enhance agricultural yields.

Characterization of Fermentation Products. The production of polysaccharides and rhamnolipids by the original seven disease-suppressive bacteria was studied from liquid-state cultures, and the physical properties of the resulting supernatants were determined (Table 1). The biomass produced after 72 h in standard succinate medium (SSM) broth ranged between 1.12 and 1.86 g/L, with isolates FQA PB-3 and GRP_3 producing maximum biomass. SHIU-13 showed the highest level of polysaccharides followed by isolate 146 and GRP_3. Maximum polysaccharide/biomass ratio was also calculated for isolates SH1U-13 (0.433), followed by isolate 146, FQP PB-3, and GRP_3.

Rhamnolipid quantification was assessed after 120 h incubation at 28 °C in PPGAS medium.[16] Significantly, GRP_3 produced the highest level of rhamnolipids (0.041 g/L) and showed the largest rhamnolipid/biomass ratio. It showed a high emulsification index value (62.7) and the maximum lowering of the surface tension (from 78 nM/m to 45 nM/m) of all the isolates studied (Table 1).

Secondary Metabolites. Identically prepared methanol extracts of bacterial cultures, grown in SSM broth, were rapidly screened

* To whom correspondence should be addressed. Tel: 0049 531-6181-7200. Fax: 0049 531-6181-7099. E-mail: victor.wray@helmholtz-hzi.de.
[†] Department of Structural Biology, HZI.
[‡] Research Group Microbial Drugs, HZI.
[§] GB Pant University of Agriculture & Technology.

10.1021/np0700016 CCC: $37.00
Published on Web 05/19/2007

Table 1. Biophysical Characterization of Polysaccharide and Rhamnolipid Production in Select Bacterial Isolates after 120 h in PPGAS Broth[a]

bacterial isolate	final pH[b]	biomass W (g/L)	polysaccharide M (g/L)	M/W ratio	rhamnolipid R (g/L)	R/W ratio	final surface tension[b]	emulsification index E_{24}
146	8.32 ± 0.04	1.28 ± 0.10	0.49 ± 0.05	0.383	$<(0.5 \pm \text{na}) \times 10^{-3}$	<0.0004	58 ± 4.36	24.4 ± 4.19
D4	8.40 ± 0.06	1.48 ± 0.08	0.18 ± 0.04	0.122	$<(0.5 \pm \text{na}) \times 10^{-3}$	<0.0004	69 ± 6.25	3.7 ± 0.76
H3	8.20 ± 0.09	1.12 ± 0.07	0.25 ± 0.06	0.223	$(1.0 \pm 0.27) \times 10^{-3}$	0.0009	64 ± 6.56	15.4 ± 2.76
SH1U-13	6.45 ± 0.05	1.20 ± 0.10	0.52 ± 0.06	0.433	$(12.1 \pm 1.61) \times 10^{-3}$	0.0100	69 ± 7.21	68.5 ± 6.27
FQP PB-3	8.20 ± 0.04	1.26 ± 0.09	0.37 ± 0.05	0.294	$(26.3 \pm 2.48) \times 10^{-3}$	0.0206	51 ± 2.65	72.7 ± 7.38
FQA PB-3	8.21 ± 0.09	1.86 ± 0.06	0.21 ± 0.03	0.113	$<(0.5 \pm \text{na}) \times 10^{-3}$	<0.0004	64 ± 4.36	6.4 ± 0.92
GRP_3	8.23 ± 0.05	1.76 ± 0.07	0.47 ± 0.05	0.267	$(41.4 \pm 1.59) \times 10^{-3}$	0.234	45 ± 5.20	62.7 ± 7.44

[a] All values are means ± SD of three replicates. na not analyzed. [b] Initial pH and surface tension of the medium was 7.0 and 78 mN m^{-1}, respectively.

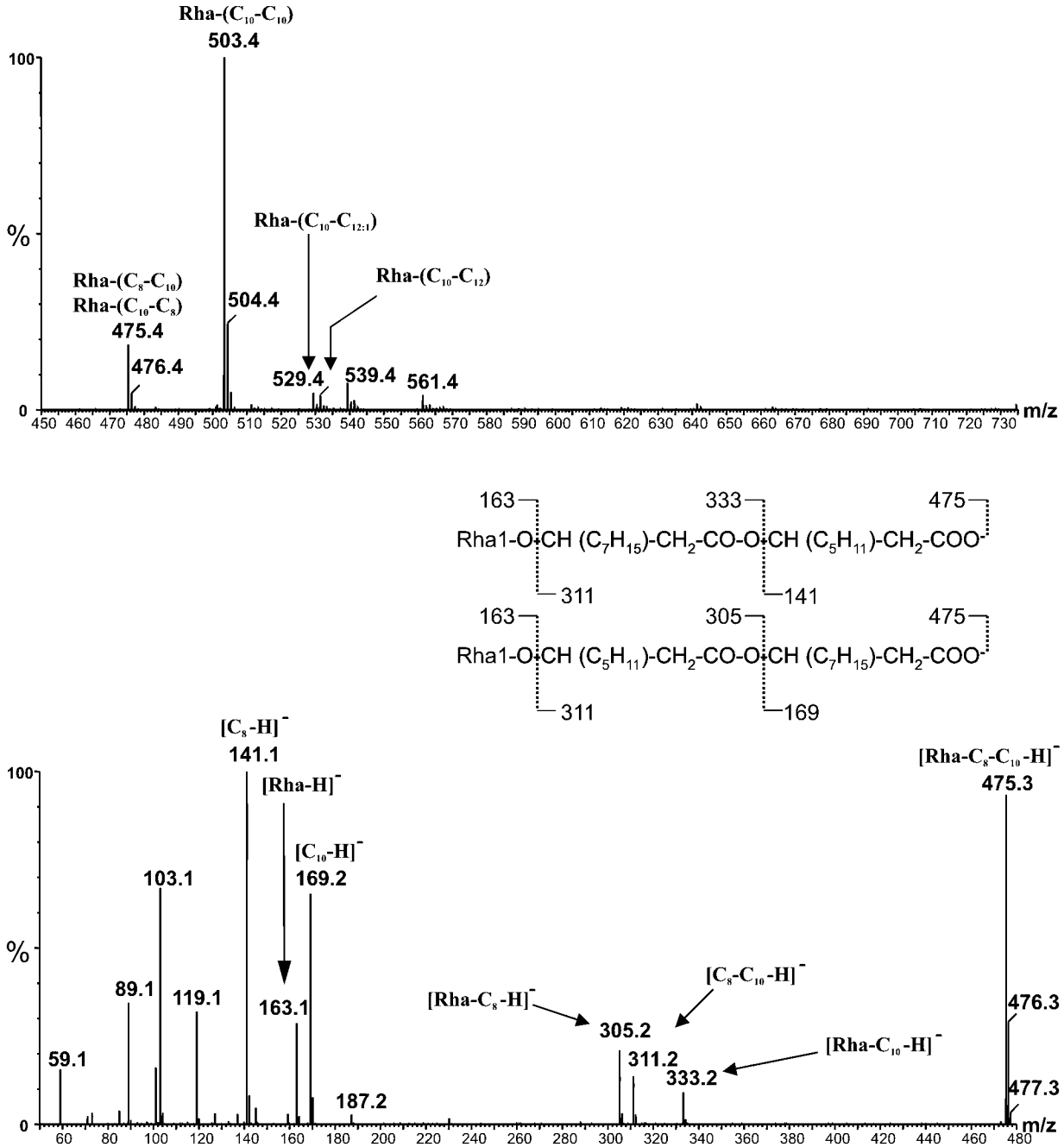

Figure 1. Negative-ion mode ESIMS of the combined monorhamnolipid fractions 7−10 after preparative TLC of XAD-16 purified sample of *Pseudomonas* sp. GRP_3. Negative-ion mode ESIMS-MS of the molecular ion at *m*/*z* 475 in. The detected fragments that allow characterization of both isomers, Rha-(C_8-C_{10}) and Rha-(C_{10}-C_8), are shown in the fragmentation scheme (lower panel).

by ^{1}H NMR spectroscopy for the presence of rhamnolipids. In all cases, apart from GRP_3, the spectra were complex and showed bands of overlapping signals in the region 5 to 0.5 ppm and in some cases (H3 and SHIU-13) significant amounts of aromatic signals in the region 9 to 6.5 ppm (Supporting Information, Figure 1). In the case of GRP_3, the spectrum appeared to be a simpler mixture with sharp bands of signals in both the sugar region 5.5 to 3 ppm and alkyl chain region 2.6 to 0.8 ppm; this was clearly

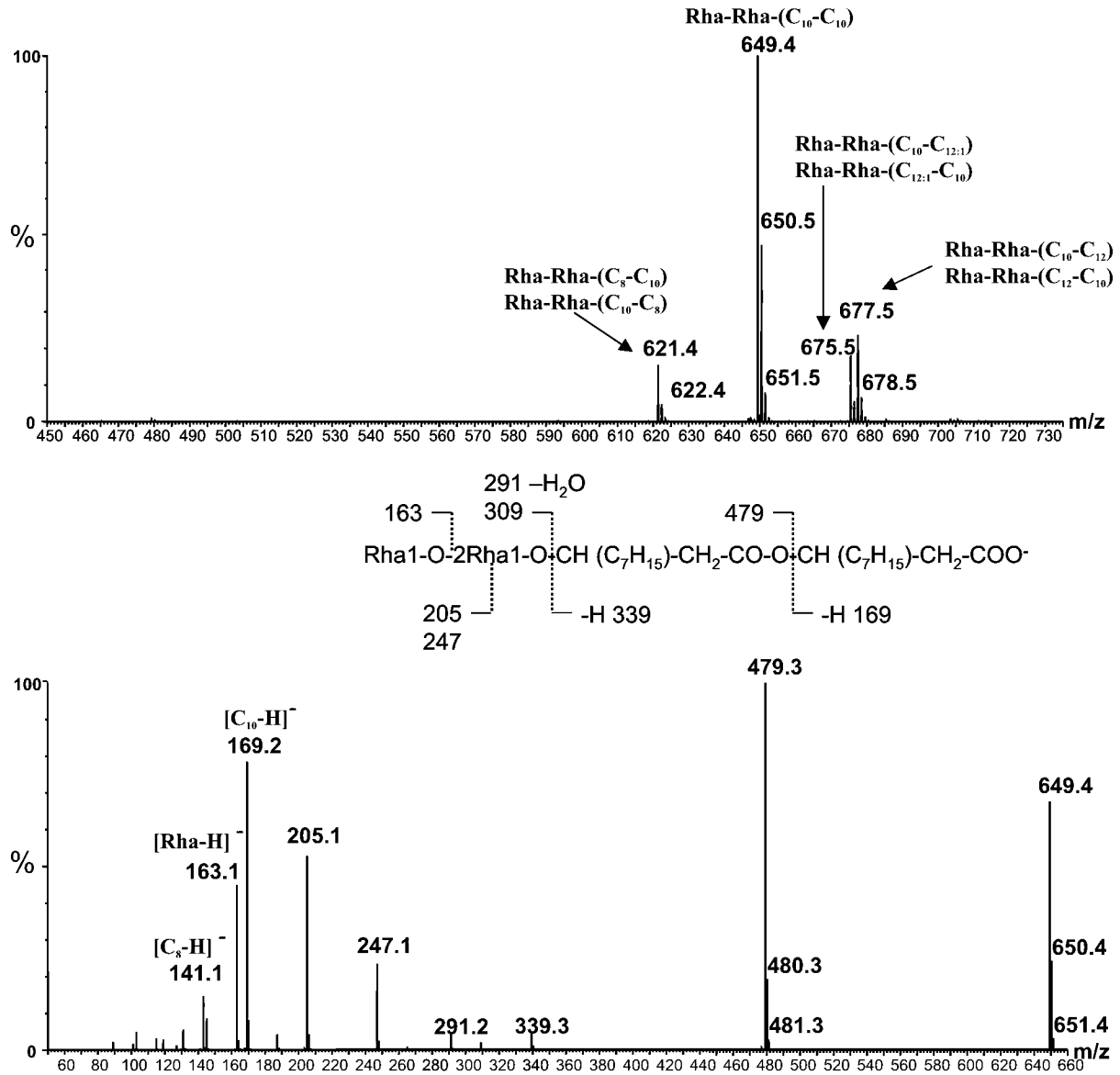

Figure 2. Negative-ion mode ESIMS of the combined dirhamnolipid fractions 15−18 after preparative TLC of XAD-16 purified sample of *Pseudomonas* sp. GRP_3. Negative-ion mode ESIMS-MS of the molecular ion at *m*/*z* 649 (detected fragments and their *m*/*z* values) is shown in the fragmentation scheme at the top of the figure (lower panel).

indicative of a sample rich in glycolipids that were probably rhamnolipids from the strong characteristic methyl doublet at 1.3 ppm (Supporting Information, Figure 2). The concentration of rhamnolipids in other extracts was below detectable levels in the extracts of the other six isolates, so the presence of rhamnolipids could not be confirmed.

On the basis of the above, a XAD-16 purified sample of GRP_3 was chosen for a more detailed component analysis. A sample of the methanol−chloroform extract of GRP_3 (430 mg) was separated by preparative TLC and analyzed under UV (at 256 and 366 nm) and visible light. Twenty fractions were identified on the preparative TLC plate and were carefully scraped and collected separately. Each fraction was eluted and evaporated to dryness. All fractions were analyzed by 1D and 2D NMR spectroscopy, which allowed a categorization of the major compounds (Table 2; Supporting Information, Figure 3) into either aromatic-containing compounds (fractions 1 to 10) or glycolipid compounds (fractions 8 to 20).

Of these, fraction 17 provided the maximum yield (11.4 mg), and the nature of the rhamnolipids present was analyzed by a combination of NMR spectroscopy and mass spectrometry. The identity of the sugar and lipid moieties and their interconnection in the major component, **2** (2-O-α-L-rhamnopyranosyl-α-L-rhamnopyranosyl-α-hydroxydecanoyl-α-hydroxydecanoic acid), were resolved by 1D and 2D homo- and heteronuclear NMR spectroscopy. The presence of characteristic spin systems corresponding to the two α-rhamnose and two α-hydroxy fatty acid moieties was readily identified from the 1D and 2D ^{1}H COSY spectra. In particular the sugar anomeric configurations follow from the small vicinal ^3J(HH)'s and ^1J(CH)'s of 170.5 Hz.[17] Their interconnection and sequence was then unambiguously determined from the cross-peaks in the 2D ^{1}H-detected multiple-bond ^{13}C−^{1}H correlation (HMBC) corresponding to interactions through three bonds via bridging oxygen atoms (Table 2). The same spectrum afforded an unambiguous assignment of the ^{13}C signals and a ready distinction between the two carbonyl carbons.

The identity of the monorhamnolipid, **1**, in fraction 10 was evident from a comparison of the 1D and 2D COSY ^{1}H NMR data with that of the **2**. In the 2D COSY spectrum only one rhamnose moiety was evident, and the characteristic signal of H-2 of the dirhamnolipid at 4.02 ppm was absent, while the characteristic signals of both fatty acid moieties were present (Table 2). In both **1** and **2** it is assumed that all sugar moieties have the normal

Table 2. NMR Data of Rhahmnolipids in CD_3OD

		dirhamnolipid			monorhamnolipid
	no.	δ_H (m, *J* in Hz)	δ_C	HMBC (δ_H to δ_C)[c]	δ_H (m, *J* in Hz)
A	1		174.3 (C)		
	2	2.61 (m)	39.9 (CH_2)	A-1	2.53 (m)
	3	5.29 (pentet, 6.4)	72.3 (CH)	**B-1**, **A-1**	5.34 (m)
	4	1.66 (m)	35.0 (CH_2)		1.65 (m)
	5−9	1.34 (m)	CH		1.34 (m)
	10	0.94 (t, 6.3)	14.4 (CH_3)		0.94 (t, 6.3)
B	1		172.4 (C)		
	2A	2.61 (m)	41.3 (CH_2)	B-1, B-3	2.61 (dd, 15.1, 7.3)
	2B	2.52 (dd, 15.2, 5.8)		B-1, B-3	2.51 (dd, 15.1, 5.4)
	3	4.09 (pentet, 6.1)	75.4 (CH)	**B-1**, **C-1**	4.13 (p, 6.1)
	4	1.58 (m)	34.3 (CH_2)		1.61 (m)
	5−9	1.34 (m)	CH		1.34 (m)
	10	0.94 (t, 6.3)	14.4 (CH_3)		0.94 (t, 6.3)
C	1	4.97 (bs)	99.2 (CH)[e]	**B-3**, C-2, C-3, C-5	∼4.80 (bs)
	2	3.79 (bs)	80.4 (CH)		3.79 (bs)
	3	3.79−3.66 (m)	71.9 (CH)		3.73−3.69 (m)
	4	3.49 (dd, 9.5, 9.5)	74.3[b] (CH)		∼3.35
	5	3.79−3.66 (m)	70.1 (CH)		3.73−3.69 (m)
	6	1.29[a] (d, ∼6)	18.0 (CH_3)	C-4, C-5	1.29 (d, 6.2)
D	1	4.93 (d, 1.5)	104.2 (CH)[e]	**C-2**, D-2, D-3, D-5	
	2	4.02 (dd, 1.5, 3.3)	71.9 (CH)		
	3	3.79−3.66 (m)	72.3 (CH)		
	4	3.49 (dd, 9.5, 9.5)	73.9[b] (CH)		
	5	3.79−3.66 (m)	70.2 (CH)		
	6	1.28[a] (d, ∼6)	18.0 (CH_3)	D-4, D-5	

[a,b]Interchangeable. [c]Bold carbons indicate sequential correlations. [d]Signals at 32.9, 32.9 (t × 2 A8, B8), 30.7, 30.4, 30.3, 30.2 (t × 4, A6, B6, A7, B7), 26.2, 25.8, (t × 2, A5, B5), 23.6 (t, A9, B9). [e]In both cases $^1J(CH) = 170.5$ Hz from the residual coupling in the HMBC spectrum.

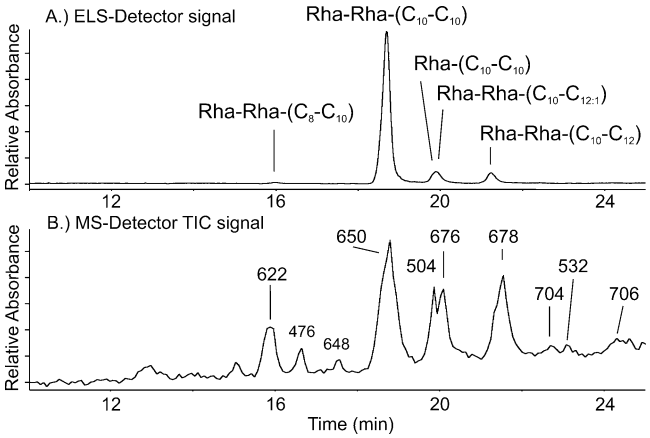

Figure 3. Quantitation of rhamnolipids from XAD-16 purified extract of *Pseudomonas* sp. GRP_3. HPLC analysis using an evaporative light-scattering (ELS) detector (A) instead of the mass spectrometric total ion current (TIC) detection (B) clearly indicates Rha-Rha-(C_{10}-C_{10}) is the predominant rhamnolipid produced by *Pseudomonas* sp. GRP_3.

absolute L-configuration. Although integration of the 1D spectra gave some idea of the length of the fatty acid chains in both types of molecules, their exact lengths were deduced from the MS data below.

The presence of rhamnolipids in the crude extract was detected by ESI^+MS, and the exact nature of these in selected glycolipid-containing fractions was analyzed by $ESI^{\pm}MS$ (Q-TOF) and HPLC-ESI^-MS (qqq) (Table 3). The data showed that fractions 7−12 comprised monorhamnolipids of different chain lengths with saturated and unsaturated fatty acids. The main components

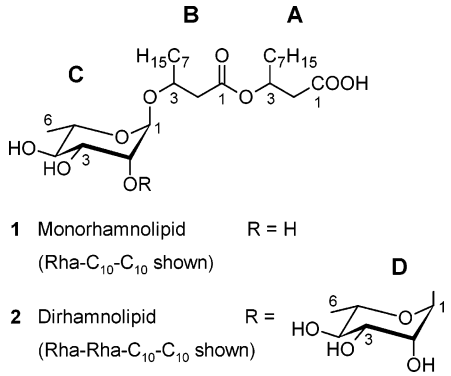

appeared as sodiated molecular ion clusters in the ESI^+MS and their structures were confirmed by MS-MS analyses. Sodiated molecular ions, $[M + Na]^+$, in the ESI^+MS data were observed at *m/z* 555 (Rha-C_{10}-C_{12}, Rha-C_{12}-C_{10}), 553 (Rha-$C_{12:1}$-C_{10}, Rha-C_{10}-$C_{12:1}$), 527 (Rha-C_{10}-C_{10}), and 499 (Rha-C_{10}-C_8, Rha-C_8-C_{10}), where Rha indicates a rhamnose moiety. Confirmatory negative mode HPLC-MS data confirmed these results and additionally showed the presence of small amounts of Rha−C_{10}−$C_{10:1}$, Table 3.

Fractions 15−20 provided dirhamnolipid sodiated molecular ion clusters in the ESI^+MS, while (−)-HPLC-MS confirmed the presence of dirhamnolipids in fractions 15−18. ESI^+MS data showed *m/z* 729 (Rha-Rha-C_{12}-C_{12}), 727 (Rha-Rha-C_{12}-$C_{12:1}$), 701 (Rha-Rha-C_{10}-C_{12}), 699 (Rha-Rha-C_{10}-$C_{12:1}$), 673 (Rha-Rha-C_{10}-C_{10}), and 645 (Rha-Rha-C_8-C_{10}). The mass values of the main components are given in bold numerals in Table 3. More detailed information about the structures of the rhamnolipids was derived by ESI^-MS-MS, which confirmed the presence of both possible isomers of Rha-C_{10}-C_8/Rha-C_8-C_{10} (Figure 1), Rha-Rha-C_{10}-$C_{12:1}$/Rha-Rha-$C_{12:1}$-C_{10} and Rha-Rha-C_{10}-C_{12}/Rha-Rha-C_{12}-C_{10} (Figure 2). According to the intensities of the fragment ions, the shorter fatty acid is found preferentially (by at least a factor of 2) directly linked to the rhamnose moiety in GRP_3. Finally, the structure of the various components were confirmed by an ESI^-MS-MS study of the combined mono- and dirhamnolipid fractions. (Additional mass spectra are available in the Supporting Information, Figures 3−6.) Each fraction was characterized by NMR spectroscopy and the various mass spectrometric techniques. The combined data from fragmentation in ESI^+MS-MS and those from (−)-HPLC-MS allowed the rhamnolipid content of each fraction to be rapidly assessed and showed this combination of techniques to be a very efficient tool for the detailed analysis of complex rhamnolipid mixtures after a simple TLC separation. Similar strategies have been employed previously in which the older FAB ionization MS methods have been used[18,19,20−23] that are now being superseded by the more versatile ESIMS.[24−26] The MS-MS techniques allowed us to distinguish isomeric mono- and dirhamnolipids. This is in keeping with the results of Schenk et al.,[27] who used HPLC to characterize the rhamnolipid mixture from *P. aeruginosa* DSM 2659 and also demonstrated quantification of chromatographically unresolved molecules. For example, in this study, very similar and coeluting isomers of Rha-C_8-C_{10}/Rha-C_{10}-C_8, of Rha-C_{10}-C_{12}/Rha-C_{12}-C_{10}, and of Rha-C_{10}-$C_{12:1}$/Rha-$C_{12:1}$-C_{10} of strain GRP_3 were easily distinguished (Table 3).

A simple quantitative determination of the rhamnolipid content of GRP_3 using the TLC fractions was not possible, as the samples were not pure enough. However, HPLC analysis of an extract of GRP_3 (Figure 3) using an evaporative light-scattering detector (ELS) instead of the mass spectrometer total ion current furnished a chromatogram that clearly indicates that Rha-Rha-C_{10}-C_{10} is the predominant rhamnolipid in GRP_3 (18.6 min; 87%). A smaller, later-eluting peak (20 min; 9.7%) contains about equal amounts of the main monorhamnolipid Rha-C_{10}-C_{10} and the dirhamnolipid Rha-Rha-(C_{10}, $C_{12:1}$), while the last peak (21.2 min; 7.3%) corresponds

Table 3. Identification and Characterization of TLC Fractions of Secondary Metabolites from *Pseudomonas* sp. GRP_3 Using Nuclear Magnetic Resonance (NMR) Spectroscopy and Mass Spectrometry (MS)

		major compound by NMR		major compounds by ESI$^+$MS (Q-TOF)		major compounds by (−)-HPLC-MS (qqq)	
fraction	wt (mg)	glycolipid	other compounds	$[M + Na]^+$ *m/z*	substance	$[M - H]^-$ *m/z*	substance
7	0.8		aromatic system	687			
				555	Rha-(C_{10}-C_{12}) Rha-(C_{12}–C_{10}) (MSMS)		
				553	Rha-(C_{10}-$C_{12:1}$) Rha-($C_{12:1}$-C_{10}) (MSMS)		
				527	Rha-(C_{10}-C_{10})		
				413	octyl phathalate[b]		
8	2.0		aromatic system	527	Rha-(C_{10}-C_{10})	**503**	Rha-(C_{10}-C_{10})
						529	Rha-(C_{10}-$C_{12:1}$)
						531	Rha-(C_{10}-C_{12})
9	1.4	monorhamnolipids	aromatic system	555		531	Rha-(C_{10}-C_{12})
				553		529	Rha-(C_{10}-$C_{12:1}$)
				527	Rha-(C_{10}-C_{10})	**503**	Rha-(C_{10}-C_{10})
						501	Rha-(C_{10}-$C_{10:1}$)
				499	Rha-(C_8-C_{10})	**475**	Rha-(C_8-C_{10})
10	1.5	monorhamnolipids	aromatic system	555		531	Rha-(C_{10} -C_{12})
						529	Rha-(C_{10}-$C_{12:1}$)
				527	Rha-(C_{10}-C_{10})	503	Rha-(C_{10}-C_{10})
						501	Rha-(C_{10}-$C_{10:1}$)
				499	Rha-(C_8-C_{10}) Rha-(C_{10}-C_8) (MSMS)	475	Rha-(C_8-C_{10})
11	0.9	monorhamnolipids		**527**	Rha-(C_{10}-C_{10})		
				499	Rha-(C_8-C_{10})		
				413	Octyl phathalate		
12	0.8	monorhamnolipids	glycerol + fat	527	Rha-(C_{10}-C_{10})		
				413	octyl phathalate		
13	<0.5	NA[c]		NA		NA	
14	1.0	monorhamnolipids	glycerol + fat	413	octyl phathalate	503	Rha-(C_{10}-C_{10})
				527	Rha-(C_{10}-C_{10})		
15	2.3	dirhamnolipds	glycerol + fat	729	Rha-Rha-(C_{12}-C_{12})		
				727	Rha-Rha-(C_{12}-$C_{12:1}$)	703	Rha-Rha-(C_{12}-$C_{12:1}$)
				701[a]	Rha-Rha-(C_{10}-C_{12})	**677**	Rha-Rha-(C_{10}-C_{12})
				699	Rha-Rha-(C_{10}-$C_{12:1}$)	**675**	Rha-Rha-(C_{10}-$C_{12:1}$)
				673	Rha-Rha-(C_{10}-C_{10})	649	Rha-Rha-(C_{10}-C_{10})
				413	octyl phathalate		
16	5.3	dirhamnolipds (unsaturated)				705	Rha-Rha-(C_{12}-C_{12})
						703	Rha-Rha-(C_{12}-$C_{12:1}$)
				701[a]	Rha-Rha-(C_{10}-C_{12}) Rha-Rha-(C_{12}-C_{10}) (MSMS)	**677**	Rha-Rha-(C_{10}-C_{12})
				699	Rha-Rha-(C_{10}-$C_{12:1}$) (MSMS)	**675**	Rha-Rha-(C_{10}-$C_{12:1}$)
				673	Rha-Rha-(C_{10}-C_{10})	**649**	Rha-Rha-(C_{10}-C_{10})
						647	Rha-Rha-(C_{10}-$C_{10:1}$)
17	11.4	dirhamnolipds		701	Rha-Rha-(C_{10}-C_{12})	677	Rha-Rha-(C_{10}-C_{12})
				695		675	Rha-Rha-(C_{10}-$C_{12:1}$)
				673	Rha-Rha-(C_{10}-C_{10})	**649**	Rha-Rha-(C_{10}-C_{10})
						647	Rha−Rha-(C_{10}-$C_{10:1}$)
				645	Rha-Rha-(C_8-C_{10})	**621**	Rha-Rha-(C_8-C_{10})
18	2.9	dirhamnolipds		701	Rha-Rha-(C_{10}-C_{12})	**677**	Rha-Rha-(C_{10}-C_{12})
						675	Rha-Rha-(C_{10}-$C_{12:1}$)
				673	Rha-Rha-(C_{10}-C_{10})	**649**	Rha-Rha-(C_{10}-C_{10})
				645	Rha-Rha-(C_8-C_{10})	**621**	Rha-Rha-(C_8-C_{10})
19	1.6	dirhamnolipids		695			
				673	Rha-Rha-(C_{10}-C_{10})		
				645	Rha-Rha-(C_8-C_{10})		
				503			
20	3.1	NA		**673**	Rha-Rha-(C_{10}-C_{10})		
				645	Rha-Rha-(C_8-C_{10})		
				413	octyl pathalate		

[a] MS-MS analysis showed Rha-Rha-(C_{10}-C_{12})/Rha-Rha-(C_{12}-C_{10}) about 3:1 (*m/z* 701) and Rha-Rha-(C_{10}-$C_{12:1}$) exclusively exists as an isomer, where the double bond is in the outer C12 unit. [b] Octyl phthalate is a common impurity that is generated by plastic containers. Data shown in bold represent major components of the corresponding fraction. [c] NA = data not available.

to Rha-Rha-(C_{10},C_{12}). A small peak at 16 min was identified by MS as Rha-Rha-(C_{10}-C_8) (1.1%).

Thus GRP_3 produces predominantly the dirhamnolipid Rha-Rha-C_{10}-C_{10}. In addition smaller quantities of Rha-Rha-C_8-C_{10}, Rha-Rha-C_{10}-$C_{10:1}$, Rha-Rha-C_{10}-C_{12}, Rha-Rha-C_{10}-$C_{12:1}$, and Rha-Rha-C_{12}-$C_{12:1}$ were detected, as well as monorhamnolipids with two fatty acids (Rha-C_8-C_{10}, Rha-C_{10}-C_8, Rha-C_{10}-C_{10}, Rha-C_{10}-C_{12}, Rha-C_{12}-C_{10}, Rha-C_{10}-$C_{12:1}$, Rha-$C_{12:1}$-C_{10}) (Table 3). All the rhamnolipids contained two fatty acid moieties. Unsaturated $C_{10:1}$ and $C_{12:1}$ fatty acid residues were observed, which appeared exclusively in the outer acid position of the dirhamnolipids, but in both positions in the monorhamnolipids (Table 3). The same trends have been observed previously for *P. aeruginosa* 47T2 grown on waste frying oil.[25] In general, the principal (and sometimes only) rhamnolipids considered to be produced by *P. aeruginosa* are Rha-Rha-C_{10}-C_{10} and Rha-C_{10}-C_{10}.[28−30] These appear to be particularly characteristic since other rhamnopilid producers, such as *Burkholderia pseudomallei* (formally *P. pseudomallei*), excrete different length lipid chains

as main components.[31] Arino et al.[32] reported the rhamnolipid profile of *P. aeruginosa* GL1, which produced a variety of mono- and dirhamnolipids containing one or two 3-hydroxy fatty acid residues when grown with glycerol as carbon source. Rhamnolipids with two fatty acid and one or two rhamnose moieties represented 90% of all rhamnolipids. The fatty acids were predominantly C_{10}, along with some C_8 and C_{12}.[19] Variations in the minor components are to be expected however, as the exact nature of the rhamnolipids appears to depend on isolation and fermentation conditions.[22,33]

Although the comprehensive ^{1}H NMR data of the 20 TLC fractions showed the presence of various different aromatic compounds in the sample from GRP_3, it was not possible to unambiguously identify the compounds because of the limited quantity available and the presence of contaminants.

In conclusion a comprehensive rhamnolipid profile of *Pseudomonas* sp. GRP_3 has been obtained, which may be used in the future to understand complex phenomena such as quorum sensing, community dynamics, and various other microbe−plant pathogen interactions. Clearly structure−function analyses are warranted to provide critical answers concerning the role of the different rhamnolipid components in lysis of zoospores of damping-off pathogens *in situ* and *in vitro*.

Experimental Section

General Experimental Procedures. The culture broth was centrifuged using a Sigma 3K30 centrifuge. The absorbance was recorded using a Beckman DU-640 spectrophotometer. The surface tension of culture supernatants was measured on a Fisher Autotensiomat model-21 (Fisher Science Co., Pittsburgh, PA). For secondary metabolite production bacteria were grown under controlled conditions on a rotatory shaker (Adolf Kuhner AG, Schweiz). HPLC-MS data were obtained on a HP 1100 system coupled to a PE SCIEX API 2000 LC/MS/MS system with an electrospray ionization interface. ESIMS and MS-MS data were recorded on a QTOF-II instrument (Micromass, Manchester, U.K.). 1D and 2D NMR spectra were recorded on either Bruker DPX300, ARX 400, or DMX600 NMR spectrometers.

Bacterial Culture. Bacterial cultures of seven isolates (*Pseudomonas* sp. 146, D4, H3, FQP PB-3, FQA PB-3, GRP_3 and isolate SH 1U-13), identified from our initial screening of the departmental culture collection at Pantnagar (originally isolated from samples from the Central Himalayan region), were maintained in modified King's B agar and stored as glycerol stocks at −80 °C.[9]

Biomass Determination. Actively grown (12 h) bacterial cultures were inoculated in SSM broth[9] and incubated at 28 °C and 120 rpm for 72 h on a rotatory shaker (120 rpm; 50 mm shaking diameter). Culture broth was centrifuged (20000*g*) for 10 min, the pellet was suspended in distilled water, and the contents were recentrifuged. Biomass was determined by weighing the pellet after drying at 105 °C for 24 h.

Polysaccharide Determination. After removal of the cell pellet, the supernatant was treated with three volumes of MeOH. The resulting precipitate was removed, dried at 105 °C for 4 h, and weighed.

Quantification of Rhamnolipids. Actively grown bacterial isolates were inoculated in 100 mL of PPGAS broth (16) and incubated at 28 °C at 120 rpm for 120 h. Culture broth was centrifuged (20000*g*) for 10 min, and the rhamnolipid content was estimated as rhamnose equivalents in the culture supernatant by the orcinol method.[34] Absorbance was measured at 420 nm with rhamnose as the standard.

Surface Tension Measurement. The surface tension of culture supernatants was measured on a Fisher autotensiomat. Measurements were made on supernatant samples after centrifugation. To determine surface tension, the mass of 1 drop of liquid was calculated and the radius of the drop was measured. Surface tension was calculated as

$$\mathrm{ST} = \frac{m(g)}{3.8(r)}$$

where m = mass of one drop, g = 9.8 m s^{-2}, and r = radius of the drop.

Emulsification Measurements. To determine emulsifier activity, 4 mL of centrifuged culture supernatant was added to 6 mL of kerosene oil.[35] The contents were vortexed at high speed for 2 min, and the mixture was allowed to settle for 24 h before the height of the emulsion and total height of the mixture were measured. The emulsification index (E_{24}) was calculated as

$$E_{24} = \frac{\text{height of the emulsion}}{\text{total height}} \times 100$$

Secondary Metabolite Production. For large-scale metabolite production, bacteria were grown in 2 L (10-fold 200 mL medium in 500 mL Erlenmeyer flasks) of SSM with shaking (120 rpm; 50 mm shaking diameter) at 28 °C for 42 h. Cells were harvested by centrifugation at 10000*g* for 20 min (Sigma 3K30). The supernatant was filtered through a membrane filter (0.22 μm, Millipore) to remove any bacterial cells before it was lyophilized to half the volume. The concentrated supernatant was acidified with HCl (2 M) to pH 2.0 and allowed to stir with the neutral adsorber resin Amberlite XAD-16 (1.0%) for 4 h. The supernatant was removed, and the XAD-16 was washed twice with an equal volume of distilled H_2O (HPLC grade). XAD-16 was extracted twice with an equal volume of MeOH−$CHCl_3$ (1:1 v/v) at 35 °C. The MeOH−$CHCl_3$ extracts were combined and evaporated to dryness *in vacuo*, yielding crude extract for preliminary NMR analysis and further TLC purification.

Thin-Layer Chromatography (TLC). Thin-layer chromatography was carried out on Si gel G_{254} plates (Merck). The lyophilized samples (300 mg) were dissolved in MeOH and applied to TLC plates. Before development, plates were exposed to an atmosphere of NH_3-wet filter paper in a glass chamber for 5−7 min. $CHCl_3$−CH_3OH−NH_3 (65:35:5 v/v) was used as solvent system. After drying, 20 visible zones were identified under UV light (254 and 366 nm) and marked. The Si gel from each zone was carefully scraped out and ground before each fraction was eluted with CH_2Cl_2−MeOH (70:30 v/v). All fractions were evaporated to dryness.

HPLC-Mass Spectrometry. The HPLC-MS system equipped with a solvent gradient system was used (automatic injector, column oven 40 °C), DAD-UV-detector; column Nucleodur 100-5 C18 EC, 125/2 mm (Macherey-Nagel); particle size 5 μm; solvent A = H_2O with 5% CH_3CN, B = CH_3CN with 5% H_2O, each with NH_4OAc buffer (0.5 mM) adjusted to pH 5.5 with ~40 μL/L CH_3COOH; gradient 15% B for 2 min, increasing to 90% B in 30 min; flow rate 0.3 mL/min. Mass spectra were recorded in the negative mode.

Mass Spectrometric Characterization of Glycolipids. The presence and structure of the major glycolipids were determined by analysis of both positive and negative ion electrospray mass spectra of the molecular ions and their fragmentation patterns in MS-MS spectra. Samples were dissolved in MeOH (concentration approximately 10 ng/μL), and 1−3 μL of this solutions was applied to gold-coated nanospray glass capillaries placed orthogonally in front of the entrance hole of the instrument. Approximately 1000 V was applied to the capillary, and the ions were separated by the time-of-flight analyzer. The instrument was calibrated using Na_nI_{n-1} clusters in positive and Na_nI_{n+1} clusters in negative mode. For MS-MS experiments parent ions were selected by the quadrupole mass analyzer and subjected to collision-induced dissociation (ID) (collision gas, argon; collision energy, 20−40 eV). Resulting daughter ions were then separated by the TOF analyzer.

Nuclear Magnetic Resonance (NMR). One-dimensional [^{1}H, ^{13}C, and DEPT-135] and two-dimensional [COSY, ^{1}H-detected one-bond (HMQC), and long-range (HMBC) ^{13}C−^{1}H correlations] NMR spectra were recorded at 300 K on NMR spectrometers locked to the major resonance of CD_3OD. Chemical shifts are given relative to the residual methanol signal (^{1}H, 3.35 ppm; ^{13}C, 49.0 ppm).

Acknowledgment. This work was supported by Grant No. BT/PR955/PID/24/38/98 to B.N.J. from the Department of Biotechnology, New Delhi, which is gratefully acknowledged. A Junior Research Fellowship from the University Grants Commission, New Delhi, and from the HZI (formely GBF), Braunschweig, to A.S. is gratefully acknowledged.

Supporting Information Available: This material is available free of charge via the Internet at http://pubs.acs.org.

References and Notes

(1) Johri, B. N.; Sharma, A.; Virdi, J. S. *Adv. Biochem. Eng. Biotechnol.* **2003**, *84*, 49−89.

(2) Compant, S.; Duffy, B.; Nowak, J.; Clement, C.; Barka, E. A. *Appl. Environ. Microbiol.* **2005**, *71*, 14951−4959.
(3) Glick, B. R. *Can. J. Microbiol.* **1995**, *41*, 109−117.
(4) Weller, D. M. *Annu. Rev. Phytopathol.* **1988**, *26*, 379−407.
(5) Duffy, B. K.; Defago, G. *Appl. Environ. Microbiol.* **1999**, *65*, 2429−2438.
(6) Baehler, E.; Bottiglieri, M.; Péchy-Tarr, M.; Maurhofer, M.; Keel, C. *J. Appl. Microbiol.* **2005**, *99*, 24−38.
(7) Meyer, J. M. *Arch. Microbiol.* **2000**, *137*, 135−142.
(8) Sharma, A.; Johri, B. N.; Sharma, A. K.; Glick, B. R. *Soil Biol. Biochem.* **2003**, *35*, 887−894.
(9) Picard, C.; Di Cello, F.; Ventura, M.; Fani, R.; Guckert, A. *Appl. Environ. Microbiol.* **2000**, *66*, 948−955.
(10) Stanghellini, M. E.; Miller, R. M. *Plant Dis.* **1997**, *81*, 4−12.
(11) Moulin, A. P.; Anderson, D. W.; Mellinger, M. *Can. J. Soil Sci.* **1994**, *74*, 219−228.
(12) Islam, M. T.; Hashidoko, Y.; Deora, A.; Ito, T.; Tahara, S. *Appl. Environ. Microbiol.* **2005**, *71*, 3786−3796.
(13) Sharma, A.; Wray, V.; Johri, B. N. *Arch. Microbiol.* **2007**, *187*, 321−335.
(14) Pathak, A.; Sharma, A.; Johri, B. N. *Int. Rice Res. Notes* **2004**, *29*, 35−36.
(15) Tripathi, M.; Johri, B. N.; Sharma, A. *Curr. Microbiol.* **2006**, *52*, 390−394.
(16) Zhang, Y.; Miller, R. M. *Appl. Environ. Microbiol.* **1992**, *58*, 3276−3282.
(17) Hansen, P. E. *Prog. NMR Spectrosc.* **1981**, *14*, 175−296.
(18) Bosch, M. P.; Parra, J. L.; Manresa, M A.; Ventura, F.; Rivera, J. *Biomed. Environ. Mass Spectrom.* **1989**, *18*, 1046−1051.
(19) de Koster, C. G.; Vos, B.; Versluis, C.; Heerma, W.; Haverkamp, J. *Biol. Mass Spectrom.* **1994**, *23*, 179−185.
(20) Gunther, N. W., IV; Nunez, A.; Fett, W.; Solaiman, D. K. Y. *Appl. Environ. Microbiol.* **2005**, *71*, 12288−2293.
(21) Manso Pajarron, A.; de Koster, C. G.; Heerma, W.; Schmidt, M.; Haverkamp, J. *Glycoconjugate J.* **1993**, *10*, 219−226.
(22) Rendell, N. B.; Taylor, G. W.; Somerville, M.; Todd, H.; Wilson, R.; Cole, J. *Biochim. Biophys. Acta* **1990**, *1045*, 189−193.
(23) Soberon-Chavez, G.; Lepine, F.; Deziel, E. *Appl. Microbiol. Biotechnol.* **2005**, *68*, 718−725.
(24) Benincasa, M.; Abalos, A.; Oliveira, I.; Manresa, A. *Antonie Van Leeuwenhoek* **2004**, *85*, 1−8.
(25) Haba, E.; Pinzo, A.; Jauregui, O.; Espuny, M. J.; Infante, M. R.; Manresa, A. *Biotechnol. Bioeng.* **2003**, *81*, 316−322.
(26) Lepine, F.; Deziel, E.; Milot, S.; Villemur, R. *J. Mass Spectrom.* **2002**, *37*, 41−46.
(27) Schenk, T.; Schuphan, J.; Schmidt, B. *J. Chromatogr. A* **1995**, *693*, 7−13.
(28) Lang, S.; Wullbrandt, D. *Appl. Microbiol. Biotechnol.* **1999**, *51*, 22−32.
(29) Maier, R. M.; Soberon-Chavez, G. *Appl. Microbiol. Biotechnol.* **2000**, *54*, 625−633.
(30) Ochsner, U. A.; Reiser, J.; Fiechter, A.; Witholt, B. *Appl. Environ. Microbiol.* **1995**, *61*, 3503−3506.
(31) Häussler, S.; Nimtz, M.; Domke, T.; Wray, V.; Steinmetz, I. *Infect. Immun.* **1998**, *66*, 1588−1593.
(32) Arino, S.; Marchal, R.; Vandecasteele, J. P. *Appl. Microbiol. Biotechnol.* **1996**, *45*, 162−168.
(33) Deziel, E.; Lepine, F.; Dennie, D.; Boismenu, D.; Mamer, O. A.; Villemur, R. *Biochim. Biophys. Acta* **1999**, *1440*, 244−252.
(34) Chandrasekaran, E. V.; Bemiller, J. N. *Methods Carbohydr. Chem.* **1980**, *8*, 89−96.
(35) Cooper, D. G.; Goldenberg, B. G. *Appl. Environ. Microbiol.* **1987**, *53*, 224−229.

NP0700016